Food & Function

PAPER

View Article Online
View Journal | View Issue

Cite this: *Food Funct.*, 2019, **10**, 5853

Gymnemic acid alleviates inflammation and insulin resistance *via* PPARδ- and NFκB-mediated pathways in db/db mice

Yumeng Li,[a,b] Yao Xiao,[a] Wenge Gao,[a] Jiahui Pan,[a] Qi Zhao[a] and Zesheng Zhang *[a,b]

Received 1st July 2019,
Accepted 8th August 2019

DOI: 10.1039/c9fo01419e

rsc.li/food-function

Gymnemic acid (GA) is a naturally occurring herbal ingredient that improves glucose metabolism in patients with diabetes mellitus. In this study, we evaluated the ameliorative effects of GA on obesity-induced inflammation and insulin resistance (IR), and identified the mechanisms for these effects in db/db mice. In these mice, GA effectively lowered fasting blood glucose concentrations from 26.3 ± 4.09 to 17.4 ± 3.38 mmol L^{-1}, and improved oral glucose and insulin tolerance. Furthermore, GA treatment accelerated lipid transport and promoted fatty acid oxidation, which reduced lipid accumulation and inhibited expression of inflammatory cytokines, including those involved in the proliferator-activated receptor δ (PPARδ)- and nuclear factor κB (NFκB)-mediated signaling pathways. In addition, the anti-inflammatory effects increased the ratio of insulin to glucagon. It also regulated the insulin signal transduction with reduced phosphorylation of IRS-1 (Ser) and increased phosphorylation of IRS (Tyr) in liver, skeletal muscle and adipose tissue. In summary, we demonstrated in db/db mice that GA induces fatty acid oxidation, and alleviates inflammation and IR in liver, skeletal muscle and adipose tissue through PPARδ- and NFκB-mediated signaling pathways.

1. Introduction

Type 2 diabetes mellitus (T2DM) is characterized by hyperglycemia and insulin resistance (IR) in peripheral tissues, and is accompanied by intracellular lipid accumulation, an inflammatory response, and pancreatic beta cell dysfunction.[1] Liver, skeletal muscle and adipose tissue are the key peripheral tissues in the body that are involved with energy metabolism and homeostasis.[2] These tissues are also known as targets for inflammation and IR.[3] It is commonly accepted that increased plasma free fatty acids (FFA) and intracellular lipid accumulation cause both inflammation and impaired insulin signaling, leading to IR through various pathways.[4,5] These signaling pathways activate a pro-inflammatory transcription factor known as nuclear factor κB (NFκB). This, in turn, stimulates expression of pro-inflammatory cytokines such as tumor necrosis factor alpha (TNFα), monocyte chemoattractant protein (MCP-1), and interleukin-6 (IL-6), which are critical in the development of IR and T2DM.[2,6] Therefore, inhibition of inflammatory signaling is of critical importance to the treatment of T2DM.

db/db (C57BL/KsJ) mice have leptin receptor point mutations that lead to leptin signaling pathway disorders. This results in complications like obesity, IR, hyperglycemia and fatty liver indicating that db/db mice are an ideal animal model of T2DM.[7,8] Adipose tissue in db/db mice increases with advancing age. Early suppression of inflammation caused by lipids is critical to alleviating IR and lowering blood glucose concentrations.

Gymnemic acid (GA) is a crude saponin fraction obtained from Gymnema sylvestre leaf extracts. GA is a natural product that has been used as a herbal remedy for thousands of years worldwide.[9,10] GA has been shown to have anti-hyperglycemic effects by reducing blood glucose concentrations in patients with T2DM.[11,12] Recent studies have also indicated that GA stimulates insulin secretion, improves insulin action and lowers blood lipid concentrations in murine models.[13,14] Our previous studies showed that GA alleviates endoplasmic reticulum stress and improves insulin signal transduction in T2DM rats and in IR HepG2 cells.[15] However, the molecular mechanism underlying the ability of GA to alleviate obesity-induced inflammation in T2DM remains unclear. In this study, we investigated the effects of GA on obesity-induced inflammation

[a]*Key Laboratory of Food Nutrition and Safety, Ministry of Education, College of Food Engineering and Biotechnology, Tianjin University of Science & Technology, Tianjin 300457, China. E-mail: zhangzesheng@tust; Fax: +86 022 6091 2431; Tel: +86 022 6091 2431*
[b]*Tianjin Food Safety & Low Carbon Manufacturing Collaborative Innovation Center, 300457 Tianjin, China*

and IR. We also explored the downstream peroxisome proliferator-activated receptor δ (PPARδ) and NFκB-mediated inflammatory pathways in db/db mice.

2. Materials and methods

2.1 Chemicals

GA (GA I–IV, 95% purity), rat insulin and glucagon ELISA kits, RIPA, nitrocellulose membranes and an SABC (rabbit IgG)-POD kit were obtained from Solarbio Science and Technology Co., Ltd (Beijing, China). A blood glucose meter and test strips were acquired from Johnson & Johnson Co. (New Brunswick, NJ, USA). Trizol was purchased from TransGen Biotech Co., Ltd (Beijing, China). Antibodies for peroxisome PPARδ, NFκB, p-NFκB-p65 (ser536), MCP-1, TNFα, IL-6, insulin receptor substrate (IRS), phospho-IRS (ser307) and phospho-IRS (tyr895), protein kinase B/Akt (Ser473), phospho-Akt, glucose transporter 2 (GLUT2) and glucose transporter 4 (GLUT4) were obtained from Cell Signaling Technology Inc. (Danvers, MA, USA). Secondary antibodies were purchased from ZSGB-BIO Technology Co., Ltd (Beijing, China). The other laboratory chemicals used in our experimental work were of analytical grade.

2.2 Animals and experiment design

Six-week old male db/db (C57BL/KsJ) mice were purchased from Sibeifu Biotechnology Co., Ltd (Beijing, China). All mice were housed individually on a 12 h light/12 h dark cycle at a temperature of 23 ± 2 °C and humidity of 55 ± 10%, with free access to water and food. The mice were allowed to adapt to these conditions for one week before the beginning of the experimental procedure. The animal procedures were approved by the Animal Care and Use Committee on the Ethics of Animal Experiments of Tianjin University of Science and Technology (Tianjin, China). All related facilities and experimental procedures were executed according to the Technical Standards for the Testing & Assessment of Health Food (2003).

2.3 GA treatment study

The db/db mice were divided into two groups (n = 10 each) according to baseline plasma glucose concentrations and body weights. GA was dissolved in distilled water, and was administered by gavage at the dose of 100 mg kg^{-1} day^{-1} as the GA dose group (db/db-GA). The second group was given the same volume of distilled water as the db/db group (db/db), and both groups were fed a normal chow diet. For eight weeks, the mice were given free access to water and food, and their body weight, food intake and fasting blood glucose (FBG) concentrations were measured weekly.

2.4 Oral glucose tolerance test (OGTT) and insulin tolerance test (ITT)

The OGTT was performed in all mice during the eighth week of treatment, as described by Zhang *et al.*[16,17] Briefly, animals were fasted for 12 h before oral administration of the vehicle (db/db group) or GA 100 mg kg^{-1} (db/db-GA group). After 20 min, all mice were given glucose 2 g kg^{-1} orally. Glucose concentrations were then determined from blood drawn from the tail tip at 0, 30, 60, 90 and 120 min. The results were expressed as the integrated area under the concentration-time curve (AUC) for glucose.

The ITT was performed as described by Zhang *et al.*[18] Briefly, animals were fasted for 8 h and then vehicle (db/db group) or GA 100 mg kg^{-1} (db/db-GA group) was administered orally. After 20 min, the mice were injected subcutaneously with insulin at a dose of 0.5 U kg^{-1}. Blood samples drawn at 0, 30, 60, 90 and 120 min after insulin injection were then used to quantitate glucose concentrations.

At the end of the eight week treatment period, mice were fasted for 8 h. After the ITT experiment, mice were anesthetized with 10% chloral hydrate (3.5 mL kg^{-1}) and sacrificed. Blood samples were collected and centrifuged (4000 rpm) at 4 °C for 15 min, and the serum stored at −80 °C before analysis. Tissues were excised immediately and then stored at −80 °C for further biochemical analyses.

2.5 Analyses of metabolic parameters

Several metabolic parameters were measured in the postmortem serum samples using commercial kits (Nanjingjiancheng, Nanjing, China) according to the manufacturer's instructions. Insulin, glucagon, triglyceride (TG), total cholesterol (TC) and FFA were measured using a sandwich-type enzyme immunoassay kit (Nanjingjiancheng, Nanjing, China). Glycated hemoglobin (HbA1c) was measured using HbA1c hemoglobin assay kits (USCN Life Science, Wuhan, China), and expressed as the ratio of HbA1c to total hemoglobin as reported by Mang *et al.*[19] The serum concentrations of TNFα, IL-6 and MCP-1 were measured using an ELISA kit (Huyu biotechnology, Shanghai, China). The liver concentrations of TG were measured using commercial kits (Nanjingjiancheng, Nanjing, China) according to the manufacturer's instructions.

2.6 Immunofluorescence staining

Immunofluorescence staining was performed as described by Zheng *et al.*[20] Briefly, isolated pancreatic tissues were fixed with 4% paraformaldehyde at 4 °C for 2 h. Tissues were then paraffin-embedded and 5 μm sections were cut. Tissue sections were incubated overnight at 4 °C with the primary antibodies. After rinsing with phosphate buffered saline, the tissues were incubated with the secondary antibodies (diluted 1 : 200) for 40 min. Immunofluorescence images were acquired using a BZ-II analyzer (Keyence, Osaka, Japan).

2.7 Determination of fecal short-chain fatty acids (SCFAs)

Fecal samples were collected once each week, and dried in a lyophilizer before being ground into a powder and weighed. SCFAs in the fecal contents were measured *via* gas chromatography with the following conditions: Agilent 7890A GC system; HP-INNO WAX column (Agilent 19091N-133; 260 °C; 30 m × 250 μm × 0.25 μm; in: back SS inlet N2; out: back detector FID) and a flame ionization detector (Agilent Technologies Inc., CA, USA).

Standard curves for the SCFAs (acetic, propionic, butyric, valeric, isobutyric and isovaleric acids) (Supelco 46975-U, Sigma) were obtained with the concentration as the abscissa (X) and the standard peak area as the ordinate (Y). Samples were prepared by dissolving fecal samples (0.1 g) into formic acid 0.9% solution (1 mL), homogenizing for 1 min and then centrifuging (13 000 rpm) for 10 min. The same volume of ethyl acetate was then added to the supernatant before shaking and mixing, extracting at 4 °C for 12 h, and centrifuging (13 000 rpm) for 10 min. The supernatant was filtered (0.22 μm filter membrane) and injected into the gas chromatography instrument.

2.8 Histopathological examination

Histopathological examination was performed as described by Li *et al.*[21] Briefly, a cubic centimeter of liver, skeletal muscle and adipose tissues was selected to fix in paraformaldehyde 4% solution for 24 h before dehydrating with different strengths of ethanol. The tissues were then embedded in paraffin, cut into 5 μm thick sections with a microtome, and stained with hematoxylin and eosin (H&E). Finally, the slides were observed under inverted microscope and the images recorded. Image pro-plus 6.0 and Image Gauge v4.0 software (fujifilm) were used to measure the number and area of adipocyte from each section.

2.9 Real-time polymerase chain reaction (RT-PCR) analysis

RT-PCR was used to determine the expression levels of target genes. Total RNA was isolated from liver, skeletal muscle and adipose tissue using Trizol reagent as per the manufacturer's protocol. cDNA was synthesized from total RNA with RT-PCR kits (Takara Biomedical Technology, Beijing, China). RT-PCR analysis was performed with premixed SYBR green reagent in a real-time detector under the following parameters: 95 °C for 30 s, followed by 40 cycles at 95 °C for 5 s and 58 °C for 5 s, with a final extension step of 72 °C for 30 min. The relative expressions of target genes were determined using the $2^{-\Delta\Delta Ct}$ method, with β-actin as an endogenous control. PCR primer sequences were designed using the Primer 5 program and are listed in Table 1.

2.10 Western blot analysis

Protein expression was assessed by western blot analysis. Briefly, 100 mg of liver, skeletal muscle and adipose tissue samples were homogenized in RIPA buffer with phenylmethanesulfonyl fluoride 1% for 10 min, followed by centrifugation (10 000 rpm) at 4 °C for 5 min. Total protein concentrations were measured *via* Bradford assays. Equal amounts of protein were separated by 10% sodium dodecyl sulfate polyacrylamide gel electrophoresis, and transferred onto polyvinylidene fluoride membranes (Millipore, Bedford, MA, USA). The membranes were incubated in blocking reagent containing 5% non-fat dried milk at room temperature for 1.5 h, and probed overnight with primary antibodies at 4 °C. Tris buffered saline tween containing anti-β-actin (1 : 10 000), anti-PPARδ (1 : 1000), anti-p-NFκB-p65 (ser536) (1 : 1000), anti-NFκB (1 : 1000), anti-MCP-1 (1 : 1000), anti-TNFα (1 : 1000), anti-IL-6 (1 : 1000), anti-phospho-IRS (ser307) (1 : 1000), anti-phospho-IRS (tyr895) (1 : 1000), anti-IRS (1 : 1000), anti-AKT (1 : 1000), anti-p-AKT (1 : 1000), anti-GLUT2 (1 : 1000) and anti-GLUT4 (1 : 1000). Membranes were then labeled with horseradish peroxidase-conjugated secondary antibodies at room temperature for 2 h. Protein expression was determined using electro-chemiluminescence and bands were visualized through autoradiography. Band intensities were quantified using ImageJ software.

Table 1 RT-PCR primer sequences

Gene	Primer	Sequences 5′–3′	NCBI number
apoE	Sense	GGGTTGGCTCCAGAAACAGA	138310.1
	Antisense	AAAGTCACACCATCCGTCCC	
CPT1a	Sense	ACTCCGCTCGCTCATTCC	013495.2
	Antisense	TTGAGGGCTTCATGGCTCAG	
CPT1b	Sense	CATGTATCGCCGCAAACTGG	009948.2
	Antisense	CCTGGGATGCGTGTAGTGTT	
ACO	Sense	GGAATCTGGAGATCACGGGC	015729.3
	Antisense	AGGCCACCACTTGATGGAAG	
ADP	Sense	GTTGCAAGCTCTCCTGTTCC	000071.6
	Antisense	CTTGCCAGTGCTGTTGTCAT	
FABP1	Sense	GGAAGGACATCAAGGGGGTG	017399.4
	Antisense	TCACCTTCCAGCTTGACGAC	
FABP3	Sense	CTCACTCATGGCAGTGTGGT	010174.1
	Antisense	GAGGGGAAAACCATGAGGCA	
FABP4	Sense	GAAATCACCGCAGACGACAG	024406.2
	Antisense	AACACATTCCACCACCAGCTT	
TLR4	Sense	GTGCCAGTCAGGGTCATTCA	021297.3
	Antisense	ACTCCCCAGCCCTTTATGGA	
TLR6	Sense	ACCGTCAGTGCTGGAAATAGA	011604.3
	Antisense	AGAGAACGGGGTCATGCTTC	
CD36	Sense	CCTTGGCAACCAACCACAAA	001159555.1
	Antisense	ATCCACCAGTTGCTCCACAC	
Fatp1	Sense	AGACTTCTGTGAGAACCTGCG	011977.3
	Antisense	TGTGCTGGAGCTTGCCTGAT	
β-Actin	Sense	GATCGATGCCGGTGCTAAGA	007393.5
	Antisense	TCCTATGGGAGAACGGCAGA	

2.11 Statistical analyses

The data are expressed as means ± standard deviation (SD) and were analyzed by SPSS16.0 software (SPSS, Chicago, IL, USA). The differences between two groups were analyzed using Student's *t*-test, and the differences among multiple groups were analyzed using one-way analysis of variance followed by the Bonferroni *post-hoc* test. $P < 0.05$ was considered statistically significant.

3. Results

3.1 Effects of GA on metabolic parameters in db/db mice

As shown in Table 2, mouse body weight and food intake were recorded weekly, with the db/db-GA group having significantly lower food intake and body weight than the db/db group at 14 w of age. Moreover, GA treatment significantly lowered liver and epididymal fat weight, and also significantly lowered TC, TG and FFA serum concentrations compared with the db/db group (Table 3). These results suggest that GA reduces lipid accumulation in metabolic tissue and lipid concentrations in

Table 2 Effect of GA on body weight and food intake of experimental mice

	Body weight (g)		Food intake (g day^{-1})	
Groups	Age (6 w)	Age (14 w)	Age (6 w)	Age (14 w)
db/db	35.2 ± 2.80	53.7 ± 1.72	5.01 ± 0.27	6.97 ± 0.12
db/db-GA	35.6 ± 1.99	45.4 ± 1.63$^{\#\#}$	5.14 ± 0.31	6.28 ± 0.25$^{\#\#}$

Data are expressed as the means ± SD (n = 10 per group), w: weeks, $^{\#\#}P < 0.01$ *vs.* db/db group.

Table 3 Effect of GA on metabolic parameters of experimental mice

Parameters	db/db (14 w)	db/db-GA (14 w)
Liver (g)	2.91 ± 0.03	2.67 ± 0.06$^{\#\#}$
Epididymis fat (g)	5.62 ± 0.21	4.88 ± 0.13$^{\#\#}$
TC (mmol L^{-1})	1.68 ± 0.17	1.04 ± 0.08$^{\#\#}$
TG (mmol L^{-1})	1.72 ± 0.09	1.02 ± 0.07$^{\#\#}$
FFA (μmol L^{-1})	632 ± 46.7	409 ± 27.4$^{\#\#}$
HbA1c (%)	11.0 ± 0.23	6.37 ± 0.81$^{\#\#}$
Insulin (pmol L^{-1})	439 ± 27.5	659 ± 36.2$^{\#\#}$
Glucagon (pmol L^{-1})	274 ± 12.9	213 ± 19.5$^{\#\#}$

Data are expressed as the means ± SD (n = 10 per group), w: weeks, $^{\#\#}P < 0.01$ *vs.* db/db group.

the circulation, and improves the symptoms of increased body weight and food intake in db/db mice.

3.2 Effects of GA on FBG, OGTT and ITT in db/db mice

As shown in Fig. 1A, FBG concentrations in the db/db-GA group were significantly lower (by 34.5%) compared with the db/db group. HbA1c was also decreased in the db/db-GA group (Table 3), indicating that blood glucose concentrations in the GA treatment group were significantly improved during the preceding few weeks compared with the db/db group.

The effects of GA on glycemic control were further confirmed by OGTT and ITT. After oral glucose (2 g kg^{-1}) administration, blood glucose concentrations in both the db/db and db/db-GA groups reached the highest level within 30 min. Blood glucose concentrations in the db/db-GA group returned to the initial value within 120 min, while the db/db group still had a persistently high concentration at this time point (Fig. 1B). In addition, the OGTT results (Fig. 1C) demonstrated a lower AUC in the db/db-GA group compared with the db/db group.

ITT tests were performed 3-days after OGTT. The results showed that, after subcutaneous insulin (0.5 U kg^{-1}), blood glucose concentrations at 30, 60, 90 and 120 min were significantly lower in the db/db-GA group compared with the db/db group (Fig. 1D and E). This indicates that GA increased glucose utilization and improved insulin sensitivity in db/db mice.

3.3 Effects of GA on liver, skeletal muscle and adipose tissue histopathological changes

Liver, skeletal muscle and adipose are crucial tissues for energy metabolism. The morphology and pathological processes of these tissues can cause various metabolic diseases. As shown in Fig. 2A, H&E staining revealed that db/db mouse liver cells had disordered arrangement and steatosis, with vacuolar appearance and increased lipid content, which

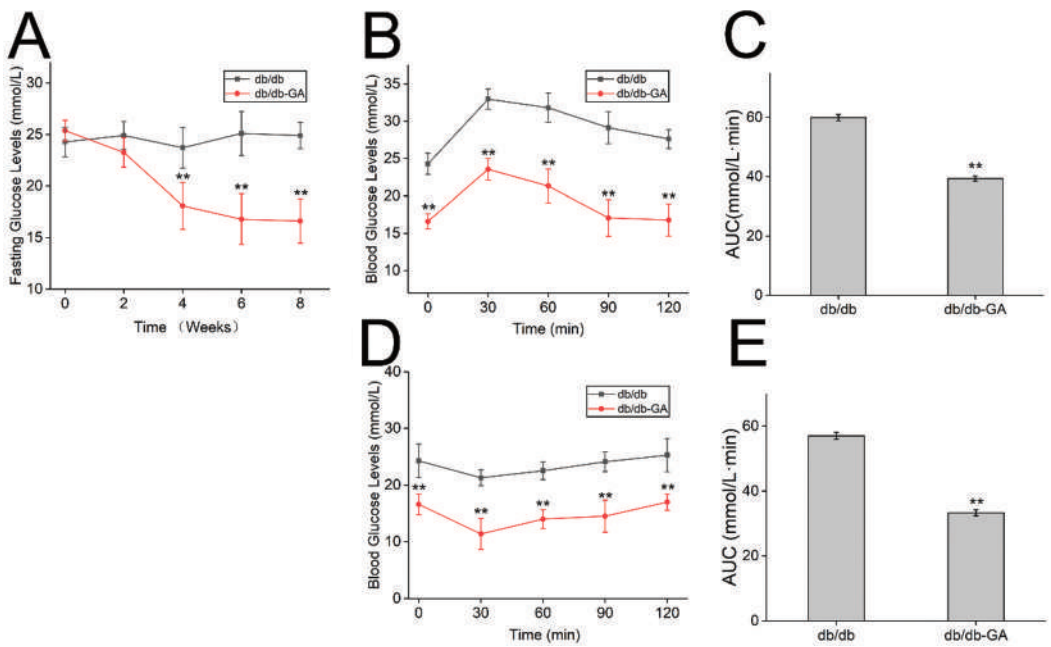

Fig. 1 Effects of GA treatment on FBG, OGTT and ITT in db/db mice. (A) FBG concentrations in the experimental mice. (B and C) OGTT was performed after 8 weeks of treatment in all experimental mice; the area under the curve of panel B was calculated and is shown in panel C. (D and E) ITT was performed in all experimental mice 3 days after OGTT; the area under the curve of panel D was calculated and is shown in panel E. Data are expressed as the mean ± SD (n = 10 per group), $^{**}P < 0.01$ *vs.* db/db group.

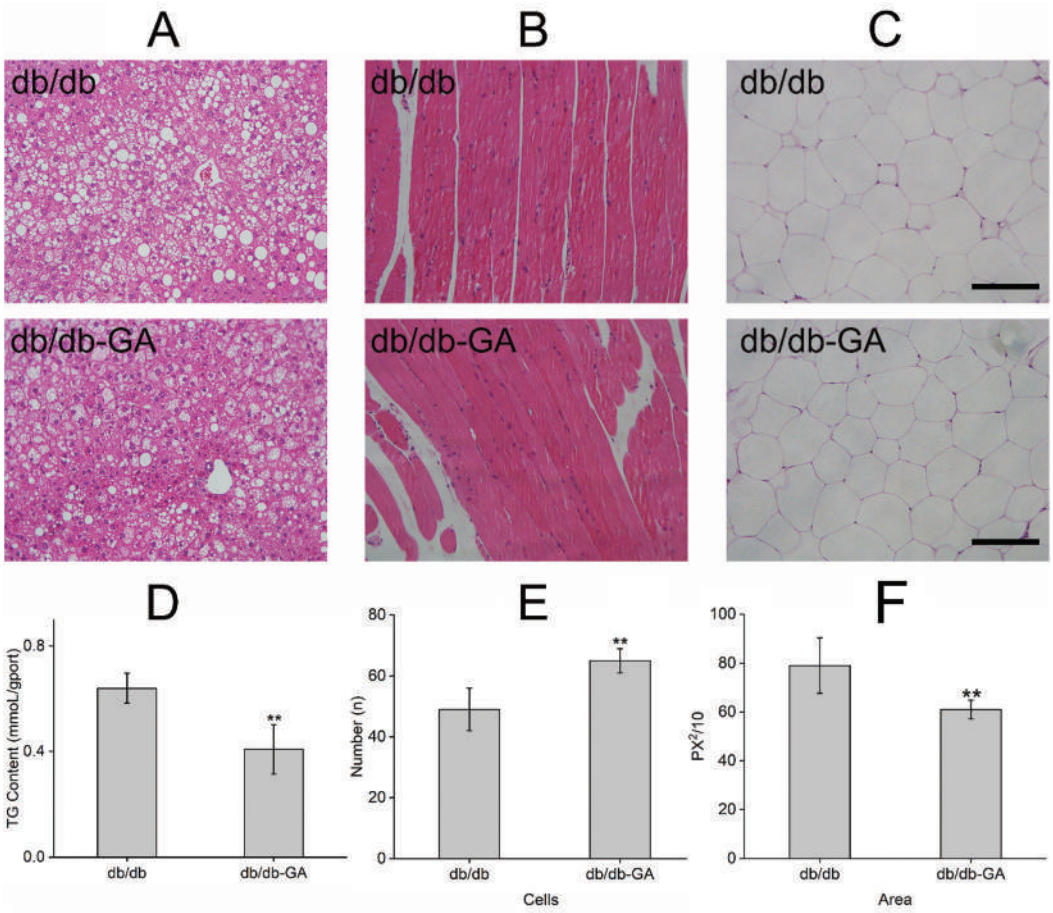

Fig. 2 Effects of GA on liver, skeletal muscle and adipose tissue histopathological change in db/db mice. (A) Histopathological change of liver. (B) Histopathological change of skeletal muscle. (C) Histopathological change of adipose; scale bar, 100 μm. (D) TG content in liver. (E) The adipocyte number in adipose section. (F) Quantification and adipocyte size measurement from adipose (eWAT) images. Values are means ± SD. Data are representative of three independent experiments, $^{**}P < 0.01$ *vs.* db/db group.

significantly improved with GA treatment. Besides, the TG content of the liver was also significantly decreased after GA treatment in db/db mice (Fig. 2D). In addition, H&E staining of skeletal muscle showed slight muscle fiber thinning in db/db mice, which was alleviated by GA treatment (Fig. 2B). Finally, morphological evaluation of adipose cells showed that the volume of these cells was enlarged in the db/db group, but was significantly decreased in the GA treatment group (Fig. 2C, E and F). These results showed that GA treatment could reduce fat accumulation and tissue lesions in peripheral tissues.

3.4 Effects of GA on expression of fatty acid oxidation genes in db/db mice

Improved lipid metabolism can reduce fat accumulation and mitigate pro-inflammatory reactions.[6] Fig. 3A–C shows that GA treatment increased the mRNA expression of fatty acid transport-associated genes, such as adiponectin (ADP) and apolipoprotein (apoE) in db/db mice. Moreover, we evaluated fatty acid oxidation-associated mRNA expression, and showed that GA administration increased carnitine palmitoyl-transferase 1 (CPT1a/b), acyl-CoA oxidase (ACO), and fatty acid binding protein 1/3/4 (FABP1/3/4) mRNA expression in the liver, skeletal muscle and adipose tissues of db/db mice.

Fig. 3D and E shows that GA treatment decreased the mRNA expression of fatty acid translocase CD36 (CD36) and fatty acid transport protein 1 (FATP1). These two proteins are involved with fatty acid transport into cells. Further, fatty acid sensing and pro-inflammatory-related genes including Toll-like receptor 4 (Tlr4) and Toll-like receptor 6 (Tlr6) are both down-regulated by GA treatment in the liver, skeletal muscle and adipose tissues of db/db mice.

3.5 Effects of GA on inflammatory markers in db/db mice

To investigate the effect of GA on inflammatory response, we evaluated inflammatory markers in the circulation and in tissues such as the liver, skeletal muscle and adipose of db/db mice. As shown in Fig. 4A–C, the serum concentrations of inflammatory cytokines (including TNF-α, MCP-1 and IL-6) were significantly lowered in the db/db-GA group. We also used western blot to assess PPARδ, NFκB, p-NFκB-p65(ser536), TNF-α, MCP-1 and IL-6 in the liver, skeletal muscle and

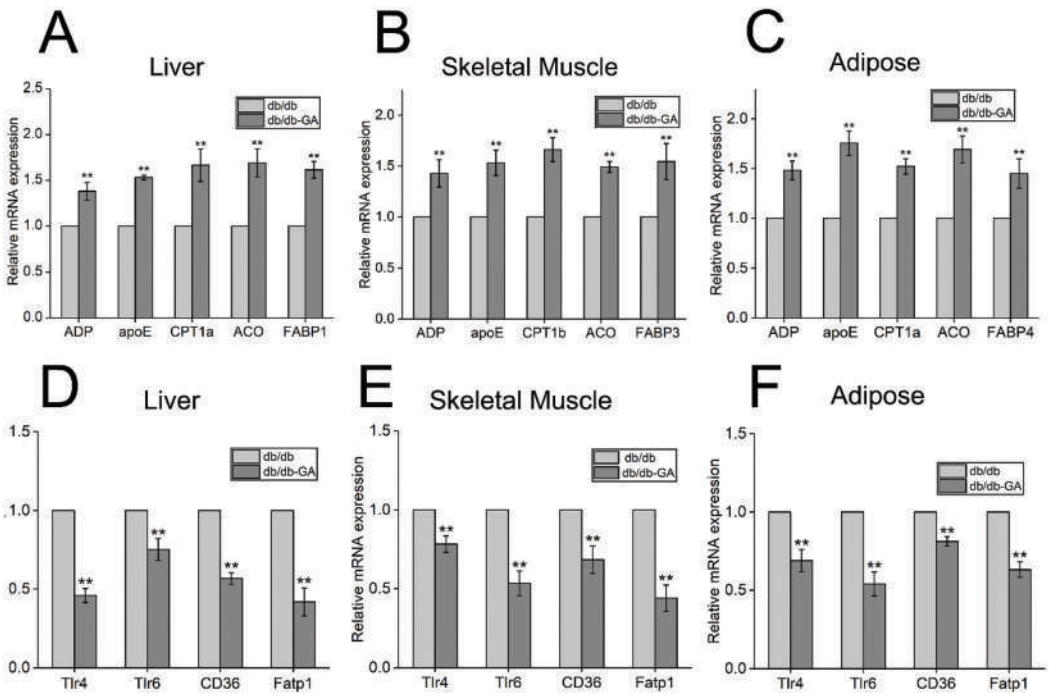

Fig. 3 Effects of GA on fatty acid metabolism genes in db/db mice. (A) Relative expression of fatty acid oxidation mRNA in liver. (B) Relative expression of fatty acid oxidation mRNA in skeletal muscle. (C) Relative expression of fatty acid oxidation mRNA in adipose. (D) Relative expression of fatty acid sensing and pro-inflammatory mRNA in liver. (E) Relative expression of fatty acid sensing and pro-inflammatory mRNA in skeletal muscle. (F) Relative expression of fatty acid sensing and pro-inflammatory mRNA in adipose. mRNA values are expressed as the fold increase relative to the db/db group after normalization to β-actin mRNA expression. Values are means ± SD. Data are representative of three independent experiments, $^{**}P < 0.01$ *vs.* db/db group.

adipose tissues of the two mouse groups. The results showed that p-NFκB-p65(ser536), TNF-α, MCP-1 and IL-6 levels in the db/db-GA group were significantly lower than in the db/db group, while PPARδ levels were significantly higher in the db/db-GA group (Fig. 4D–F). Finally, we also determined the SCFA fecal content (Fig. 4G), with GA treatment shown to increase SCFA fecal content, which was highest in the fourth week of treatment.

3.6 Effects of GA on insulin sensitivity in db/db mice

We investigated insulin signaling, to determine the effects of GA on inflammatory response and insulin sensitivity. As shown in Fig. 5A, immunofluorescence staining showed that GA treatment increased the ratio of insulin to glucagon, which was consistent with the serum insulin and glucagon content results determined by ELISA (Table 3). Additionally, proliferation of beta islet cells (the red areas represent proliferating beta cells) was significantly higher in the db/db-GA group compared with the db/db group (Fig. 5B). Based on these results, the effect of GA on the key proteins that relate to insulin signal transduction and glucose metabolism were also studied. The results showed that GA treatment increased p-Akt and p-IRS (tyr) while decreasing p-IRS (ser). Furthermore, the expression of glucose transporters such as Glut2 and Glut4 were also increased in the liver, skeletal muscle and adipose tissue of db/db mice (Fig. 5C–E).

4. Discussion

Chronic inflammation mediated by lipid accumulation is an important underlying factor in obesity-related T2DM.[22,23] db/db mice, characterized by obesity, IR, hyperglycemia and fatty liver, have been employed widely as an inflammation and obesity-associated T2DM model to evaluate the activity and mechanism of hypoglycemic drugs.[24,25] GA has been shown to display anti-diabetic activity, and our previous studies have identified that GA can alleviate endoplasmic reticulum stress in T2DM rats and in IR HepG2 cells.[26] In this study, we investigated the effect of GA on obesity-induced inflammation and IR, and its hypoglycemic mechanism in db/db mice.

Based on previous studies,[26] we selected the dose of 100 mg kg^{-1} day^{-1} to investigate the anti-diabetic effects of GA in db/db mice. After 8 weeks of GA treatment, body weight, food intake and viscera index were all decreased in the db/db-GA group, indicating that the imbalance of energy metabolism in db/db mice was regulated by GA treatment. FBG, OGTT, ITT and HbA1c are the most commonly employed indicators of diabetes, and reflect the body's glucose concentrations.[27,28] After 8 weeks of GA treatment, the FBG concentration in db/db mice decreased, while the OGTT, ITT and HbA1c indices greatly improved, suggesting that GA significantly ameliorated hyperglycemia. In addition, basic indicators of lipid metabolism were also evaluated, with TC, TG and FFA serum concen-

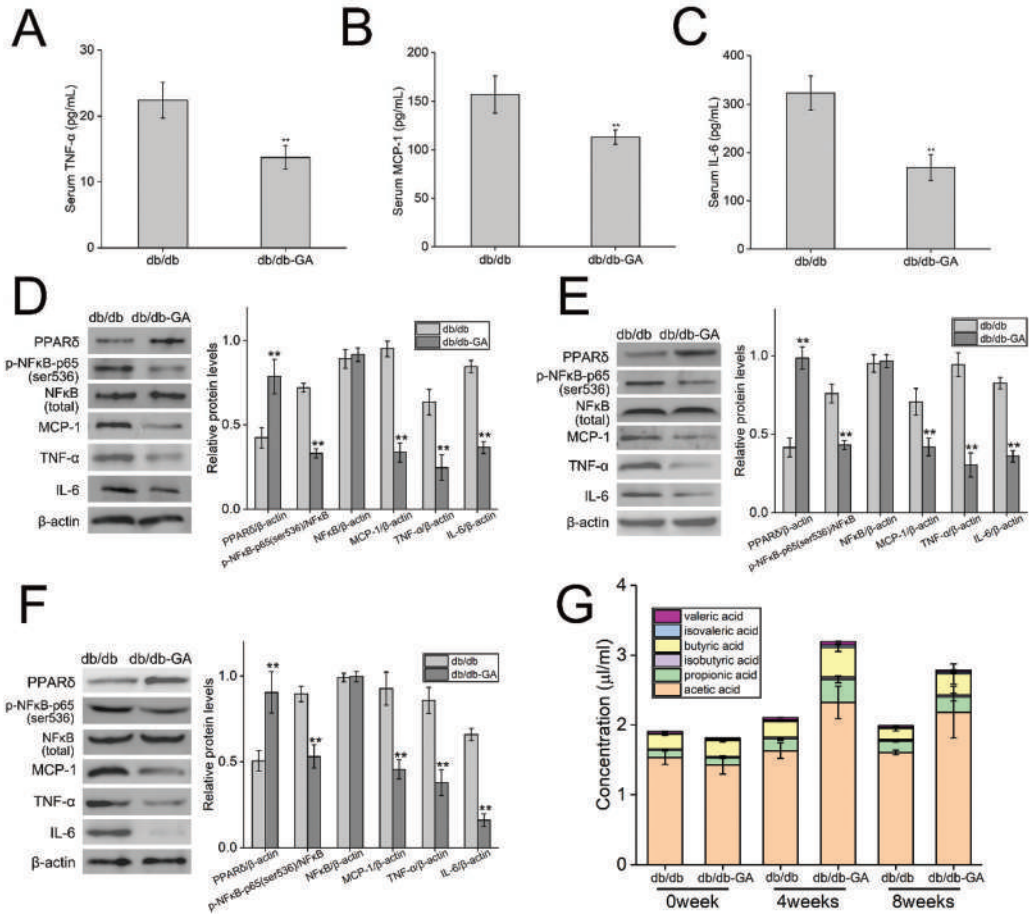

Fig. 4 Effects of GA on SCFAs and inflammatory factors in mice. (A) TNF-α concentrations in serum. (B) MCP-1 concentrations in serum. (C) IL-6 concentrations in serum. (D) Relative expression of inflammatory proteins in liver. (E) Relative expression of inflammatory proteins in skeletal muscle. (F) Relative expression of inflammatory proteins in adipose. (G) Content of SCFAs in feces. Values are means ± SD. Data are representative of three independent experiments, $^{**}P < 0.01$ *vs.* db/db group.

trations all significantly reduced after GA treatment. Taken together, these results suggest the possibility that GA may play a central role in the attenuation of IR and hyperglycemia in db/db mice. However, further studies are needed to define the mechanism for these effects.

Many studies have reported that obesity, as a chronic disease characterized by excessive accumulation of adipose tissue, increases the morbidity and mortality of IR, diabetes and cardiovascular disease.[29,30] ADP and apoE can bind and transport blood lipids to various tissues for metabolism and utilization of proteins, thereby affecting the occurrence and development of hyperlipidemia, atherosclerosis and cerebrovascular diseases. ADP concentrations predict the development of T2DM and coronary heart disease, and have shown potential in clinical trials of diabetes, atherosclerosis and inflammation. In this study, ADP and apoE mRNA expression in the liver, skeletal muscle and adipose tissue of db/db mice were obviously up-regulated by GA treatment. Further, fatty acid oxidation is an important pathway for glycerol and fatty acid metabolism *in vivo*, and can release a large amount of energy for the body to use. The mRNA expression of fatty acid oxidation-associated genes, such as CPT1a/b, ACO, and FABP1/3/4 were enhanced by GA treatment. CD36 and FATP1 are proteins that transport fatty acids into cells, and both mRNA levels are down-regulated by GA treatment. This greatly reduces the absorption of fatty acids and alleviates the metabolic burden caused by excessive lipid accumulation. These results suggest that loss of body weight and viscera index may be caused by fatty acid oxidation-mediated fat burning in peripheral tissues. This postulate is also supported by the results of H&E staining, which showed that GA treatment significantly decreased liver fatty acid content and reduced adipose cell volume. These results suggest that GA can promote the oxidation of fatty acids, thereby reducing lipid accumulation and preventing the metabolic syndrome caused by obesity.

Numerous studies have reported that diabetes and IR are often induced by inflammation.[31,32] PPARδ is an important regulator of the inflammatory response, and is a novel therapeutic target for metabolic disorders.[33] Activation of PPARδ brings many positive effects, such as weight loss, stimulation of skeletal muscle metabolic rate, and attenuation of IR.[34] PPARδ pathway activation also attenuates lipid-induced

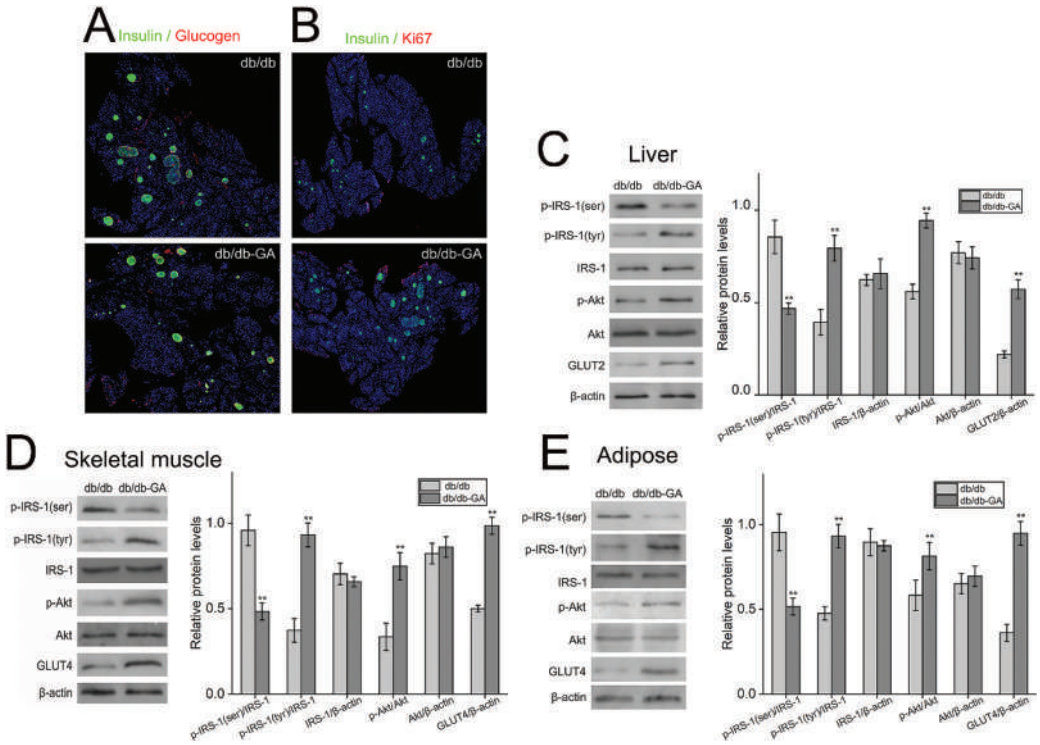

Fig. 5 Effects of GA on insulin sensitivity in db/db mice. (A) The ratio of insulin to glucagon in pancreas section; representative: insulin (green) staining, glucagon (red) staining, and nucleus of DAPI (blue) staining. (B) Proliferation of islet beta cells in pancreas section; representative: insulin (green) staining, Ki67 (red) staining, and nucleus of DAPI (blue) staining. (C) Relative expression of insulin signal proteins in liver. (D) Relative expression of insulin signal proteins in skeletal muscle. (E) Relative expression of insulin signal proteins in adipose. Values are means ± SD. Data are representative of three independent experiments, $^{**}P < 0.01$ *vs.* db/db group.

inflammation *via* suppression of NFκB-mediated signal transduction.[35] NFκB is a well-known pro-inflammatory transcription factor, which can induce IR in peripheral tissues. Activation of the NFκB mediated pathway stimulates pro-inflammatory cytokines including TNFα, IL-6 and MCP-1, which play an important role in the development of IR and T2DM. Thus, proper inhibition of lipid-induced inflammation is of great significance for the treatment of diabetes. In this study, GA treatment increased the expression of PPARδ, while decreasing a pro-inflammatory transcription factor (NFκB) and pro-inflammatory cytokines (TNFα, IL-6 and MCP-1) in the liver, skeletal muscle and adipose tissue of db/db mice. Moreover, fatty acid sensing and pro-inflammatory-related genes including Tlr4 and Tlr6 are also down-regulated by GA treatment in the liver, skeletal muscle and adipose tissues of db/db mice. SCFAs provide the main energy supply for the colonic mucosa, which can reduce production of proinflammatory factors and facilitate the repair of mucosal inflammation. In our study, GA treatment was associated with significant up-regulation of SCFA fecal content in db/db mice. Collectively, these findings demonstrate that GA treatment can increase PPARδ expression and consequently lighten the inflammatory response *via* inhibition of NFκB-mediated pro-inflammatory cytokines.

Recent major studies suggested that chronic inflammation is an important mechanism for IR and T2DM induction.[36,37] In fact, peripheral tissues are heavily infiltrated by inflammatory immune cells and excess lipid, which interact with adipocytes to trigger chronic inflammation that blocks insulin transduction.[38–40] Therefore, we investigated whether GA could promote insulin signaling by alleviating inflammation caused by lipid accumulation. Cytoplasmic IRS proteins exert important functions in the insulin activation cascade.[28] Impairment of IRS protein phosphorylation might impede the signaling cascade, leading to T2DM. Studies have demonstrated that phospho-IRS-1(ser) negatively regulates insulin receptor signaling and is a common cause of IRS-1 protein dysfunction. Moreover, decreased phospho-IRS-1(tyr) is also a risk factor for IR.[41,42] In this study, GA treatment effectively prevented damage to the insulin receptor, which is related to suppression of phospho-IRS-1(ser) and promotion of phospho-IRS-1(tyr). Further, GA treatment can also regulate key proteins related to glucose transport and metabolism, which appeared as a significant up-regulation of p-Akt and GLUT2/4 in the liver, skeletal muscle and adipose tissue of db/db mice.

In conclusion, our study demonstrates that GA ameliorates obesity-induced inflammation and IR *via* PPARδ- and NFκB-mediated signaling in the liver, skeletal muscle and adipose tissue of db/db mice. These results appear as reduced lipid accumulation and increased fatty acid metabolism, and alleviated inflammatory effects, which ultimately contribute to enhanced insulin signaling. Furthermore, our findings indi-

cate the potential of GA as a hypoglycemic agent for the treatment of obesity-associated T2DM.

Abbreviations

T2DM	Type 2 diabetes mellitus
IR	Insulin resistance
FFA	Free fatty acids
PPARδ	Peroxisome proliferator-activated receptor δ
NFκB	Nuclear factor κB
TNFα	Tumor necrosis factor alpha
MCP-1	Monocyte chemoattractant protein
IL-6	Interleukin-6
GA	Gymnemic acid
IRS	Insulin receptor substrate
Akt	Protein kinase B/Akt
GLUT	Glucose transporter
FBG	Fasting blood glucose
OGTT	Oral glucose tolerance test
ITT	Insulin tolerance test
TG	Triglyceride
TC	Total cholesterol
SCFAs	Short-chain fatty acids
ADP	Adiponectin
apoE	Apolipoprotein
CPT1	Carnitine palmitoyl-transferase 1
ACO	Acyl-CoA oxidase
FABP	Fatty acid binding protein
CD36	Fatty acid translocase CD36
FATP1	Fatty acid transport protein 1
Tlr	Toll-like receptor

Conflicts of interest

There are no conflicts of interest to declare.

Acknowledgements

This research is supported by the National Science-Technology Pillar Program (2012BAD33B05), and the Program for Changjiang Scholars and Innovative Research Team in University of the Ministry of Education of the People's Republic of China (Grant IRT1166).

References

1 T. Kiyohiko, A. Nakamura, H. Miyoshi and H. Nomoto, Effect of the Sodium – Glucose Cotransporter 2 Inhibitor Luseogliflozin on Pancreatic Beta Cell Mass in db/db Mice of Different Ages, *Sci. Rep.*, 2018, 1–11.

2 C. Angela, R. Esposito, A. Zampella, C. Festa, R. Riccio, A. Casapullo, A. Tosco and M. C. Monti, Central s-resistin deficiency ameliorates hypothalamic inflammation and increases whole body insulin sensitivity, *J. Nat. Prod.*, 2017, **90**, 9–15.

3 Z. Piotr, H. R. Hady, M. Chacinska, K. Roszczyc and J. Gorski, The Effect of High Fat Diet and Metformin Treatment on Liver Lipids Accumulation and Their Impact on Insulin Action, *Sci. Rep.*, 2018, 1–11.

4 H. Q. Li, S. Y. Peng, S. H. Li, S. Q. Liu, Y. F. Lv, N. Yang and L. Y. Yu, Chronic Olanzapine Administration Causes Metabolic Syndrome through Inflammatory Cytokines in Rodent Models of Insulin Resistance, *Nature*, 2019, 1–12.

5 K. Patthara, S. Gu, Y. X. Liu, S. Bhuvanendran and N. Gourikutty, In Vitro Micro-Physiological Model of the Inflamed Human Adipose Tissue for Immune-Metabolic Analysis in Type II Diabetes, *Nature*, 2019, 1–14.

6 S. K. Cheul, I. H. Wang, S. S. Choe, J. Park, Y. Ji, J. I. Kim and G. Y. Lee, Insulin Resistance with Adipose Tissue in flammation, *Nat. Commun.*, 2017, **40**, 122–134.

7 R. Puff, P. Dames, M. Weise, B. Göke, J. Seissler, K. Parhofer and A. Lechner, Reduced Proliferation and a High Apoptotic Frequency of Pancreatic Beta Cells Contribute to Genetically-Determined Diabetes Susceptibility of Db/Db BKS Mice, *Horm. Metab. Res.*, 2011, **43**, 306–311.

8 D. Louise, D. L. C. Almholt, T. Neerup, E. Vassiliadis, N. Vrang, L. Pedersen, K. Fosgerau and J. Jelsing, Characterisation of Age-Dependent Beta Cell Dynamics in the Male Db/Db Mice, *PLoS One*, 2013, **8**, e82813.

9 C. Guilin and M. Guo, Rapid Screening for α-Glucosidase Inhibitors from Gymnema Sylvestre by Affinity Ultrafiltration-Hplc-Ms, *Front. Pharmacol.*, 2017, **8**, 1–8.

10 A. Capolupo, R. Esposito and A. Zampella, Determination of Gymnemic Acid I as a Protein Biosynthesis Inhibitor Using Chemical Proteomics, *J. Nat. Prod.*, 2017, **80**, 909–915.

11 I. Yusuke, T. Murai, T. Imoto, M. Ohnishi, M. Oda and S. Ishijima, Gymnemic Acids Inhibit Rabbit Glyceraldehyde-3-Phosphate Dehydrogenase and Induce a Smearing of Its Electrophoretic Band and Dephosphorylation, *FEBS Lett.*, 2005, **43**, 33–36.

12 F. G. Di, V. Romanucci, A. D. Marco and A. Zarrelli, Triterpenoids from Gymnema Sylvestre and Their Pharmacological Activities †, *Nat. Commun.*, 2014, **109**, 56–81.

13 R. Barbara, C. Festa, S. D. Marino, S. D. Micco, M. V. D'Auria, G. Bifulco, S. Fiorucci and A. Zampella, Molecular Decodification of Gymnemic Acids from Gymnema Sylvestre. Discovery of a New Class of Liver X Receptor Antagonists, *Steroids*, 2015, **96**, 121–131.

14 P. Ramesh, R. K. Sharma, J. Chagalamarri and P. K. Kavadi, A Systematic Review of Gymnema Sylvestre in Obesity and Diabetes Management, *J. Sci. Food Agric.*, 2013, **94**, 834–840.

15 Y. M. Li, M. Z. Sun, Y. P. Liu, J. J. Liang, T. X. Wang and Z. S. Zhang, Gymnemic Acid Alleviates Type 2 Diabetes Mellitus and Suppresses 2 Endoplasmic Reticulum Stress in Vivo and in Vitro, *J. Agric. Food Chem.*, 2019, **67**, 3662–3669.

16 G. Shan, Q. Guo, C. G. Qin, R. Shang and Z. S. Zhang, Sea Buckthorn Fruit Oil Extract Alleviates Insulin Resistance through the PI3 K/Akt Signaling Pathway in Type 2 Diabetes Mellitus Cells and Rats, *J. Agric. Food Chem.*, 2017, **13**, 28–36.
17 G. Y. Feng, M. N. Zhang, T. X. Wang, T. C. Wu, R. D. Ai and Z. S. Zhang, Hypoglycemic Effect of D-Chiro-Inositol in Type 2 Diabetes Mellitus Rats through the PI3 K/Akt Signaling Pathway, *Mol. Cell. Endocrinol.*, 2016, **433**, 26–34.
18 G. Y. Feng, M. N. Zhang, T. C. Wu, M. Y. Xu, H. N. Cai and Z. S. Zhang, Effects of D-Pinitol on Insulin Resistance through the PI3 K/Akt Signaling Pathway in Type 2 Diabetes Mellitus Rats, *J. Agric. Food Chem.*, 2015, **60**, 19–26.
19 B. Mang, M. Wolters, B. Schmitt, K. Kelb, R. Lichtinghagen, D. O. Stichtenoth and A. Hahn, Effects of a Cinnamon Extract on Plasma Glucose, HbA 1c, and Serum Lipids in Diabetes Mellitus Type 2, *Eur. J. Clin. Invest.*, 2006, **36**, 40–44.
20 Z. G. Zheng, Y. P. Zhou, X. Zhang, P. Myat, Z. S. Xie, C. Lu and T. Pang, Anhydroicaritin Improves Diet-Induced Obesity and Hyperlipidemia and Alleviates Insulin Resistance by Suppressing SREBPs Activation, *Biochem. Pharmacol.*, 2016, **122**, 42–61.
21 J. Li, T. Wu and X. L. Lv, Function Barrier Function and Inhibits Digestive Enzyme, *Food Funct.*, 2019, **10**, 33–43.
22 H. L. Kammoun, T. L. Allen, D. C. Henstridge, S. Barre, R. C. Coll, G. I. Lancaster, L. Cron and S. Reibe, Evidence against a Role for NLRP3-Driven Islet in flammation in Db/Db Mice, *Mol. Metab.*, 2018, **10**, 66–73.
23 A. Kei, H. Yamada, H. Miyazawa, T. Minagawa, M. Nakajima, M. I. Ryder and K. Gotoh, Oral Pathobiont Induces Systemic Inflammation and Metabolic Changes Associated with Alteration of Gut Microbiota, *Sci. Rep.*, 2018, 1–11.
24 P. C. Li, Y. F. Tang, L. M. Liu, D. Wang, L. Zhang and C. H. Piao, Therapeutic Potential of Buckwheat Hull Fl Avonoids in Db/Db Mice, a Model of Type 2 Diabetes, *J. Funct. Foods*, 2019, **52**, 84–90.
25 G. D. Noratto, K. Murphy and B. P. Chew, Quinoa Intake Reduces Plasma and Liver Cholesterol, Lessens Obesity-Associated Inflammation, and Helps to Prevent Hepatic Steatosis in Obese Db/Db Mouse, *Food Chem.*, 2019, **10**, 7–14.
26 Y. M. Li, M. Z. Sun, Y. P. Liu, J. J. Liang, T. X. Wang and Z. S. Zhang, Gymnemic Acid Alleviates Type 2 Diabetes Mellitus and Suppresses 2 Endoplasmic Reticulum Stress in Vivo and in Vitro, *J. Agric. Food Chem.*, 2019, **67**, 3662–3669.
27 K. C. Ronald and S. Ussar, Regulation of Glucose Uptake and Enteroendocrine Function by the Intestinal Epithelial Insulin Receptor, *Diabetes*, 2017, **66**, 886–896.
28 O. Kentaro, M. Miyazaki, M. Matsuhisa, K. Takano, Y. Nakatani, M. Hatazaki and T. Tamatani, Insulin Resistance in Type 2 Diabetes, *Diabetes*, 2005, **54**, 57–63.
29 W. H. Tao, D. Gris, Y. Lei, S. Jha, L. Zhang, M. T. H. Huang, W. J. Brickey and J. P. Y. Ting, Fatty Acid-Induced NLRP3-ASC Inflammasome Activation Interferes with Insulin Signaling, *Nat. Immunol.*, 2011, **12**, 408–415.
30 W. Wei, Q. J. Liu, Y. Tan, L. C. Liu, X. K. Li and L. Cai, Oxidative Stress, Diabetes, and Diabetic Complications, *Hemoglobin*, 2009, **33**, 370–377.
31 M. Marie, V. Rigalleau, L. Blanco, K. Mohammedi and P. Blanco, Chronic Low Grade Inflammation in Type 2 Diabetes—Activation of the Inflammasomes by Circulating Metabolites, *Diabetes*, 2018, **67**, 22–26.
32 E. P. Brennan, M. Mohan, A. McClelland, M. de Gaetano, C. Tikellis, M. Marai, D. Crean, A. Dai, O. Beuscart, S. Derouiche, S. P. Gray, R. Pickering, M. Tan, M. Godson-Treacy, S. Sheehan, J. F. Dowdall, M. Barry, O. Belton, S. T. Ali-Shah and P. J. Guiry, Lipoxins protect against inflammation in diabetes-associated atherosclerosis, *Diabetes*, 2018, 1–42.
33 C. W. San, W. T. Wong, L. Zhao, J. Xu, L. Wang, C. W. Lau and Z. Y. Chen, PPARδ Is Required for Exercise to Attenuate Endoplasmic Reticulum Stress and Endothelial Dysfunction in Diabetic Mice, *Diabetes*, 2017, **66**, 519–528.
34 L. Yimagou, E. S. Kang, K. Zhang, A. Goyal, J. E. Young, P. Kishore, E. Rosen and M. Hawkins, Insulin Sensitizing Effects of Vitamin D Mediated through Reduced Adipose Tissue Inflammation and Fibrosis, *Diabetes*, 2018, **67**, 22–26.
35 Y. Taesik, S. A. Ham, W. J. Lee, S. I. H. Wang, J. A. Park, J. S. Hwang and J. Hur, Ligand-Dependent Interaction of PPARδ with T-Cell Protein Tyrosine Phosphatase 45 Enhances Insulin Signaling, *Diabetes*, 2018, **67**, 360–371.
36 R. J. Perry, G. Camporez, K. F. Petersen, G. I. Shulman, G. Camporez, R. Kursawe, P. M. Titchenell, D. Y. Zhang and C. J. Perry, Hepatic Acetyl CoA Links Adipose Tissue Inflammation to Hepatic Insulin Resistance and Type Article Hepatic Acetyl CoA Links Adipose Tissue Inflammation to Hepatic Insulin Resistance and Type 2 Diabetes, *Cell*, 2015, **7**, 45–58.
37 T. E. O'Sullivan, M. Rapp, X. Y. Fan, T. Walzer, A. J. Dannenberg, J. C. Sun and T. E. O. Sullivan, Adipose-Resident Group 1 Innate Lymphoid Cells Promote Obesity-Associated Insulin Resistance Article Adipose-Resident Group 1 Innate Lymphoid Cells Promote Obesity-Associated Insulin Resistance, *Immunity*, 2016, **45**, 428–441.
38 K. Maya and R. Medzhitov, Homeostasis, Inflammation, and Disease Susceptibility, *Cell*, 2015, **160**, 16–27.
39 O. N. Cristina and J. Bollerslev, The Impact of Adipose Tissue on Insulin Resistance in Acromegaly, *Trends Endocrinol. Metab.*, 2016, **27**, 26–37.
40 V. Carrera, Manuel, Unraveling the Effects of PPAR β/δ on Insulin Resistance and Cardiovascular Disease, *Trends Endocrinol. Metab.*, 2016, **27**, 319–334.
41 X. Wei, Z. P. Li, Y. Xu, Y. Yu, Q. Zhou, L. Y. Chen and Q. Wan, Autophagy Protects Human Podocytes from High Glucose-Induced Injury by Preventing Insulin Resistance, *Metabolism*, 2016, **65**, 1307–1315.
42 N. Giuseppina, G. Manno, R. Russo, D. Buccheri, S. Dell'Oglio, P. Morreale, G. Evola, G. Vitale and S. Novo, Impact of Insulin Resistance on Cardiac and Vascular Function, *Int. J. Cardiol.*, 2016, **10**, 95–99.

